CHAPTER-4

SYNTHESIS AND CHARACTERISTICS OF DIESEL SOOT AND EXPERIMENTAL METHODS OF CATALYST MATERIALS

4.1 Preparation of Diesel Soot

The soot was prepared in the laboratory by partial combustion of locally available commercial diesel (HP) in a lamp with limited supply of air, and collected on the inner walls of an inverted beaker kept over the lamp as shown in Figure 4.1 [Dhal *et al.*, 2017]. The soot was collected from the recipient walls of the beaker and then dried in an oven for overnight at 120^{o}C to remove moisture and volatile components. The dried soot was stored in an air tight bottle for further use in the experiments.

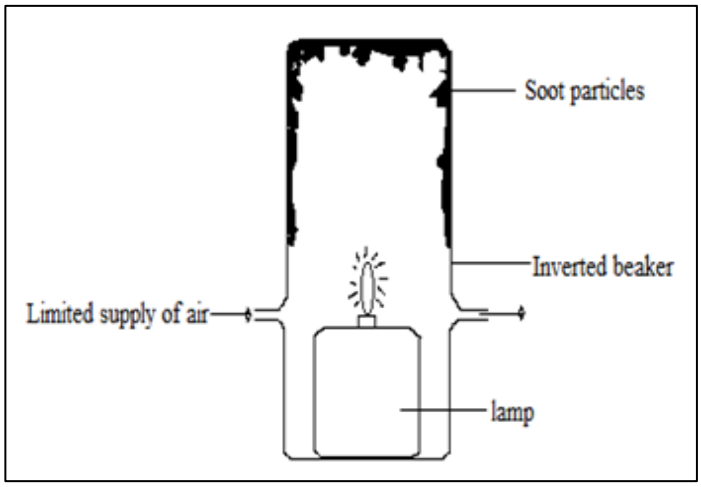

Figure 4.1 Schematic diagram of preparation of diesel soot

4.1.1 Diesel Soot Characterization

The prepared diesel soot was characterized by the following techniques: proximate analysis, Calorific value, Particle size analysis, X- ray diffraction analysis, XRD, SEM.

4.1.1.1 Proximate analysis

Proximate analysis of the laboratory prepared soot is reported in Table 4.1. The fixed carbon/VM ratio in the present study was found higher as compared to the value reported in the published paper for carbon/H_2 [Neri *et al.*, 1997]. This difference is obvious because the techniques used to characterize the soot were different, furthermore, the soot is heated the prepared soot at 200^{o}C before the performing the proximate analysis, so some of the VM is already removed from the sample. The ash content in our study was 0.1wt% is far less than 7.1wt% reported in the literature [Neri *et al.*, 1997].

Table 4.1 Proximate analysis of soot

Constituents	**wt%**
Fixed carbon	77.9
VM	21.8
Moisture	0.2
Ash	0.1

5.1.1.2 Calorific value

Calorific Value (CV) is a measure of heating power and is dependent upon the composition of the gas. The CV refers to the amount of energy released when a known weight of fuel is completely combusted under specified conditions. The calorific value of the soot was calculated using a bomb calorimeter (Table 4.2) under the following conditions: Wt. of soot taken = 0.9902 gm, Water taken in the calorimeter =1750 mL, Pressure of O_2 in the bomb = 25 kg/cm^2. Room Temperature = 28.4°C.

Table 4.2 Data obtained from bomb calorimeter

Time (min)	0	1	3	4	5	6	7	8	9	10	11
ΔT (^{o}C)	0.01	0.41	0.96	1.22	1.34	1.42	1.45	1.48	1.48	1.52	1.52

The calorific value of the soot was calculated using the Equation (4.1)

$$C_v = \{W * \Delta T – (C_{vt} + C_{vw})\}/ m \quad \text{..... (4.1)}$$

Where; W (water equivalent) = 2248 cal/ ^oC

Heat produced by combustion of thread used in the experiment (C_{vt}) = 21 Cal./gm

Heat produced by burning of fuse wire used in the experiment (C_{vw}) = 9.31 Cal./gm

Substituting the corresponding values, the calorific value of the soot was = 3397.47 Cal./gm.

4.1.1.3 Particle size analysis

Particle size analysis of the soot gives mean diameter of 1.30 μm based on particle number density, while particles of 15.25 μm occupy maximum volume based on volume density. This result is oblivious as discussed earlier section that number concentration of smaller particle is more while larger particle occupy more mass. Detail analysis is given in appendix-B.

4.1.1.4 X- ray diffraction analysis

The X-ray diffraction (XRD) pattern of diesel soot is shown in Figure 4.2 the Bragg diffraction broad peaks at 2θ= 23.68° and 42.01° are the only peaks obtained in the X-ray diffraction analysis. These two peaks correspond to hexagonal graphite lattice of multi-walled carbon nano-tubes [Malek Abbaslou *et al.*, 2010, Mi *et al.*, 2010].

The peaks at 2θ= 23.68^o is a moderately high intensity broad peak which indicates the presence of large amounts of amorphous material in association with nano-tubes. The low intensity broad peak at 2θ = 42.01°, is an indication of the amorphous carbon nano-material present in the soot. The crystallite size of the soot was estimated

to be 93.00 nm using the Scherrer equation. The crystallite size of 93.00 nm found in the present study was comparable with reported values in the literature (70-100 nm) [Kostoglou *et al.*, 2003].

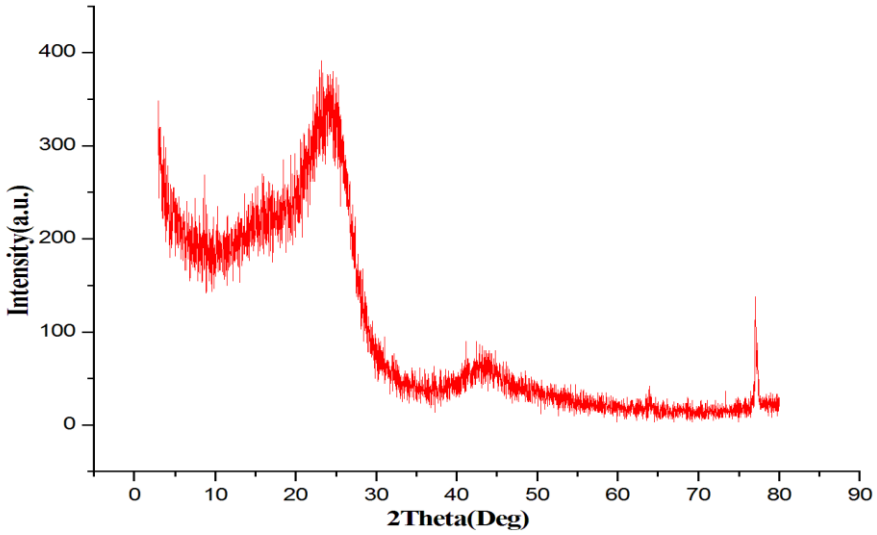

Figure 4.2 X-Ray pattern of the laboratory prepared diesel soot

4.1.1.5 Scanning Electron Microscopy

The SEM micrograph of real diesel soot is presented in Figure 4.3. The surface morphology of the soot is seen to be non-uniform. There are several grains which look like carbon nano-spheres. These sphere join together to form chains of spheres. This chain like structure is seen throughout the surface. Majority of the particle is about 0.3 μm and less.

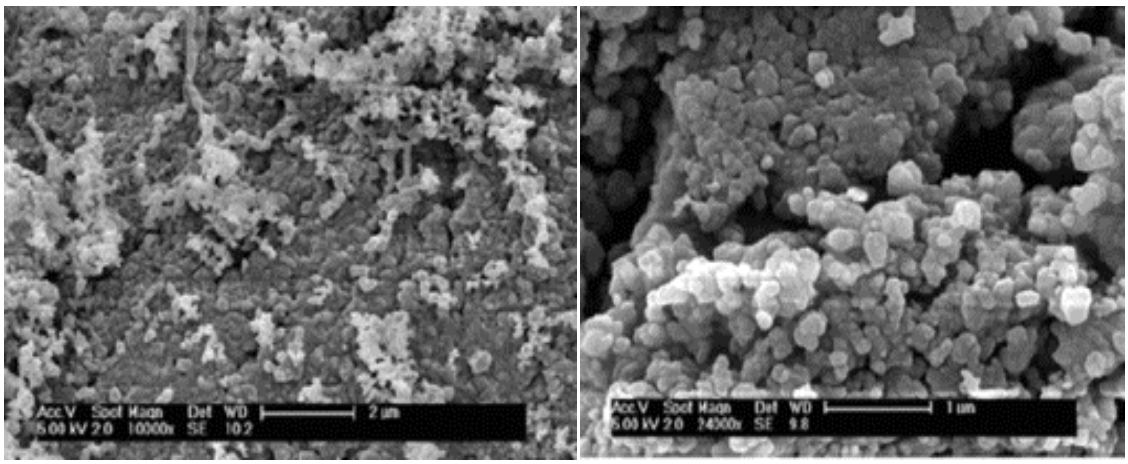

Figure 4.3 SEM images of the laboratory prepared diesel soot

4.2 MATERIALS AND EXPERIMENTAL METHODS

The Catalysts are those materials, which can accelerate or facilitate a particular chemical reaction, without undergoing any change or without being consumed in the process and hence it can be regenerated in its original form, but sometimes in a lower or higher oxidation state [Vakayil *et al.*, 2001]. Methods of catalyst preparation are very diverse and each catalyst may be produced via different routes. Preparation usually involves several successive steps. The properties of heterogeneous catalysts depend on all their previous history.

The preparation of catalysts is frequently described as an art and a catalyst recipe may specify detailed and arcane procedures that appear to be necessary in order to achieve reproducibility and desired properties. Even though the relationship between formulation procedures and ultimate catalyst behavior may in many cases be obscure, an understanding of some of the effects produced with typical catalyst ingredients by manipulations such as precipitation, washing, drying, heating etc helps to clarify the reason for suggested procedures and to indicate possible improvements in methods for preparing a specific catalyst. In all these manipulations, the usual laws different of chemistry apply, but are made more complicated by the complex nature of substances of interest.

The most important properties of a catalyst for NO reduction and Soot oxidation are its activity, selectivity and stability. To obtain reliable and meaningful results, catalysts need to be designed with utmost care. Experimental conditions must be adjusted so that the intrinsic activity of the catalyst is measured, rather than the effect of mass and heat transfer. Determination of catalytic activity is closely associated with the development of catalysts for new processes or improved formulation for practical

application. New catalysts are usually tested on a relatively small scale before putting them to a large scale. Therefore, bench scale tubular reactor has been used in this study for the measurement of the catalytic activity and for carrying out the kinetic studies.

4.2.1 Materials Required

The locally available commercial AR grade chemicals such as urea, citric acid, La $(NO_3)_3.6H_2O$, Fe $(NO_3)_3.9H_2O$, Co $(NO_3)_2.6H_2O$, $Mn(CH_3COO)_2.4H_2O$, $Cu(NO_3)_2.3H_2O$, KNO_3, KOH etc. were used in the present research work.

4.2.2 Catalysts Preparation and Methodology

The following methods were used for preparation of different perovskite catalysts and mixed metal catalysts.

a) Solution Combustion Synthesis (SCS) Method
b) Reactive Grinding Method
c) Citric acid sol-gel (SG) method

4.2.2.1 Solution combustion synthesis (SCS)

Combustion synthesis has been applied to $LaFeO_3$ production with a view to boosting its activity towards simultaneous reduction of soot and NOx process by enhancing its specific surface area (SSA), with a highly exothermic and self-sustaining reaction. This oxide can be rapidly prepared from an aqueous solution of metal nitrates (oxidizers) and urea (fuel). The favorable conditions for $LaFeO_3$ formation were sought: only fuel rich mixtures are effective, but carbonaceous deposits are formed when excess urea is used. In the field of operating conditions in which the combustion synthesis reaction takes place, the SSA were not dramatically higher than those obtained with traditional methods; moreover, even short time thermal treatments have been found to rapidly deactivate the catalysts by rapid sintering. With a view to tackling these

problems, NH_4NO_3 was selected as an additive for its low costs, highly exothermic decomposition and because it generates gaseous products only and without altering the proportion of the other elements in the catalysts. With ammonium nitrate, the specific area was enhanced from 4 m^2/g up to about 20 m^2/g followed by Civera *et al.*, 2003. A short thermal treatment at 900°C partially deactivates further the NH_4NO_3 derived catalysts. It was found that NH_4NO_3-boosted mixtures produce materials whose activity, after the similar thermal treatment, behaves practically like the perovskites obtained by the 'citrates' method. The Solution Combustion synthesis is though rather cheap in terms of reactants employed - and quick, given that the process needs few minutes at low temperature without successive calcinations [Civera *et al.*, 2003].

Combustion synthesis was carried out following the procedure described by (Biamino *et al*., 2005**)**, starting from a homogeneous liquid solution containing metal nitrates as precursors of the desired oxide and urea as sacrificial fuel. The synthesis process can be formally split into two steps. The first reaction is endothermic and represents the real perovskite synthesis in (Equation 4.2) starting from the metal nitrate precursors, while the second is exothermic and accounts for the reaction between the oxygen derived from nitrates decomposition and urea. Some direct combustion of urea with the atmospheric oxygen, of course, cannot be excluded as the preparation is carried out in air. The catalysts are then calcined in air at 600°C for 4 h to burn the carbonaceous matters as a common stabilization treatment. Taking the $LaFeO_3$ synthesis as the example, the combustion synthesis involving lanthanum nitrate, ferric nitrate and urea occurs according to the following overall reaction (Equation 4.4) which gives rise to a perovskite powder and gaseous species:

$$La(NO_3)_3 + Fe(NO_3)_3 + 5CO(NH_2)_2 \rightarrow LaFeO_3 + 5CO_2 + 8N_2 + 10H_2O \ldots (4.2)$$

The whole reaction can be formally observed as the combination of two different contributions:

$$CO(NH_2)_2 + 7.5O_2 \rightarrow 5CO_2 + 10H_2O + 5N_2 \; exothermic\; reaction \ldots\ldots\ldots (4.3)$$

$$LaNO_3 + Fe(NO_3)_3 \rightarrow LaFeO_3 + 7.5O_2 + 3N_2 \; endothermic\; reaction \ldots\ldots (4.4)$$

The exothermic reaction, namely urea combustion (Equation 4.3), provides the heat that is necessary for the completion of the decomposition, i.e., the endothermic transformation reaction of nitrate into the desired oxide. This technique is particularly suited for the production of nano-sized particles of catalyst.

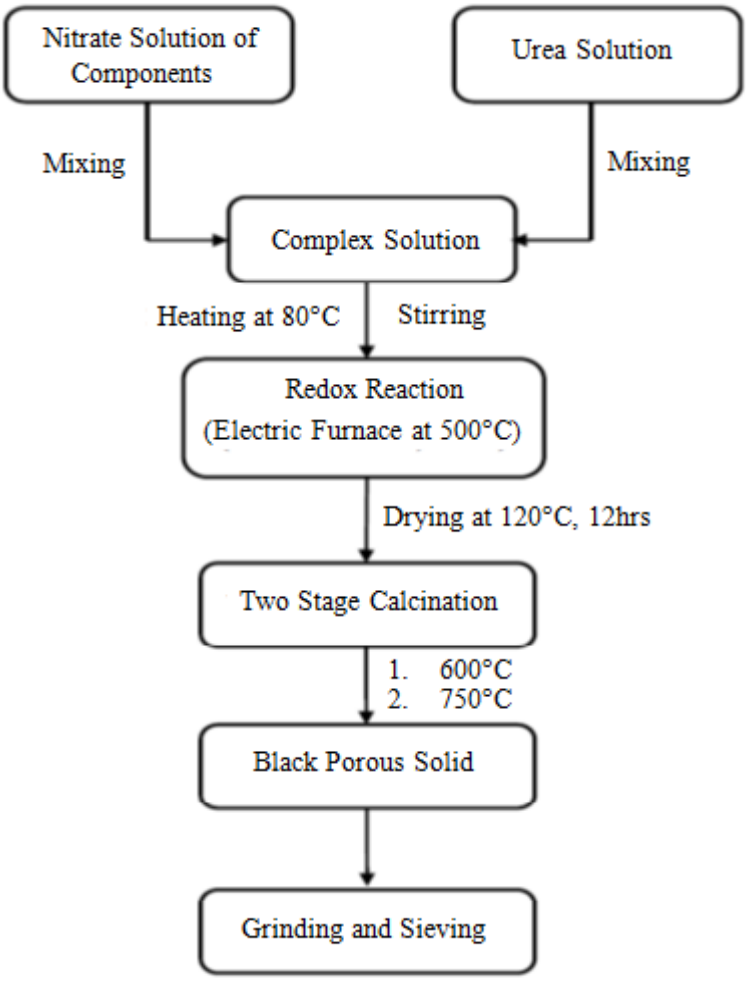

Figure 4.4 Flow diagram of SCS method

The $LaFeO_3$ catalyst was prepared in the laboratory; first, nitrate precursors was mixed with distilled water, and, after proper stirring, then 3.5 fold of stoichiometric ratio of Urea was added to the solution. Then 1g NH_4NO_3 was added to the solution and stirring it continuously up to 30 mins. When the volume was reduced to nearly 50 ml, and then calcined by 600°/4hrs in electric furnance to start the fast-sustaining redox reaction, which gave rise to a perovskite powder. Then it was grinded through mortar again calcined in for 750°C/2hrs, then after milling, final catalyst was prepared. In this way several perovskite catalysts were prepared in the laboratory as steps shown in Figure 4.4.

5.2.2.2 Reactive Grinding Method

Reactive grinding is also known as high-energy mechanical synthesis or mechano-chemical synthesis. It allows for attaining a pure perosvkite phase at room temperature without the thermal treatment. Mechanical impact during the process reduces the precursor's crystallite size to nano-scale [Patel and Patel 2012] while it provides a homogeneous mixture and enhances the solid state diffusion. The synthesis is performed in a closed environment without generating any waste [Quach *et al.,* 2011, Kaliaguine *et al.,* 2001]. The precursors with an appropriate stoichiometric ratio are mixed and ground continuously for a certain period of time in a planetary ball mill. Small balls made of YO_3 stabilized ZrO_2 and grinding jar made up of ZrO_2 are generally used in the reactive grinding method. Then the as-synthesized sample is washed with deionized water. The solid product is dried, followed by calcinations at 600°C. After grinding the calcined product, the catalyst powder is obtained. Kaliaguine *et al.,* 2001 synthesized a large variety of perovskites (ABO_3) by reactive grinding using the individual simple oxides of cations A and B as the reactants. Using various grinding

additives, high surface (measured after calcinations at 473 K) perovskites such as $LaFeO_3$ (>100m^2/g), $LaCoO_3$ (85m^2/g), $LaMnO_3$ (>80m^2/g) are consistently prepared. The additives such as zinc oxide should be leachable. ZnO is leached out of the sample using a 2M solution of ammonium chloride. Perovskite sample prepared by the reactive grinding method display a high stability of the perovskite structure under a reducing atmosphere [Huang *et al*. 2007]. Figure 4.5 shows the flow diagram of reactive grinding method.

In this method, the different perovskite catalysts were prepared by mixing by hand up to 15 mins, then grinding was done at a rotation speed of 150 rpm 4 h in a planetary ball mill with seven balls of 9 mm diameter. ZnO was added to the solution and again grinding up to 20hrs. After washing through NH_4NO_3 solution, oven drying and calcined 600°C/6hrs then after grinding in the morter final catalyst was prepared. in this way above all catalysts were prepared.

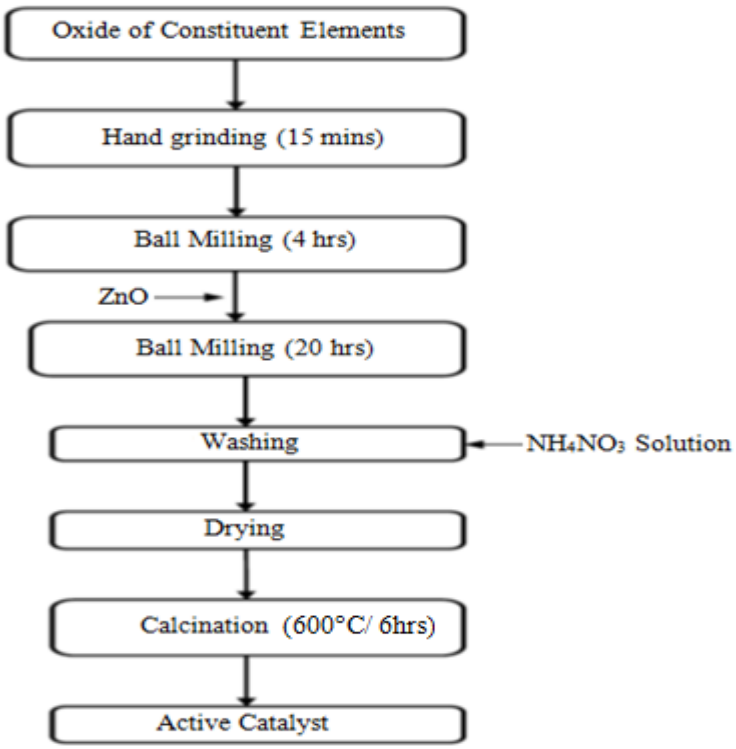

Figure 4.5 Flow diagram of reactive grinding method

In the present work, a dual drive planetary ball mill shown in Figure 4.6 (a) was used for the preparation of the catalysts. The dimensions of the jars of 67.5 mm inside diameter, outside diameter of 78 mm, height of 71.5 mm and 250 mL volume were used. The grinding balls of different diameters, 11, 9, 7 and 4 mm having weight 5.78, 3.19, 1.95 and 0.43 g respectively, made of zirconia were used. The other specifications of the planetary ball mill are such as maximum speed: 1500 rpm (variable speed from 100-1500rpm). The Jars and balls are made of zirconia and shown in Figure 4.6 (b).

Figure 4.6 (a) Planetary ball mill, (b) Jar and grinding balls (ZrO_2)

4.2.2.3 Citric acid Sol-gel (SG) method

Perovskite catalysts were prepared by a citrate sol-gel method following the procedure described by Wang *et al*., 2012. The reagents (nitrate salts of desired oxides)

first dissolved in distilled water in stoichiometric amounts. A given amount of citric acid dissolved in deionized water was added in above solution as a ligand. The solution was adjusted to pH=7.5-8.0 with aqueous ammonia or acetic acid, stirring and heating to a temperature of 60-80°C for 4 h, syrup obtained was then heated to 100°C for 24 h in air, followed by calcination at 450°C for 2 h, and then temperature was raised to 600°C in 4 h. Black samples were obtained. This method is the most effective route to create high surface area catalysts.

The $La_{0.8}K_{0.2}FeO_3$ prepared by the sol-gel method is given by Chen *et al*., 2015. Analytical grade $La(NO_3)_3.H_2O$, KNO_3 and $Fe(NO_3)_3.9H_2O$ were weighed according to the stoichiometric ratio, and then dissolved in distilled water. Some citric acid was added with the same mole fraction as for the metallic ions. The mixture was stirred for 3 h while ammonia was added to adjust the pH value to be 8-9. The mixture was dehydrated by placing in a water bath at 80-90°C. The sample slowly becomes sol, and then gels. After being heat-treated at 120°C for 2h, the sample was put into an oven at a temperature of 300-400°C for 4h, and the sample becomes powder. The powder is kept at 500°C for 2h after being further ground. Then it was calcined at 700°C for 12-24h, thus the $La_{0.8}K_{0.2}FeO_3$ perovskite composite oxide was obtained.

The $La_{0.8}K_{0.2}Fe_{0.85}Cu_{0.15}O_3$ catalyst was prepared by citric acid sol gel method [Chen *et al.,* 2015].The stoichiometric ratio of metal nitrates ($La(NO_3)_3.6H_2O$ KNO_3 and $Fe(NO_3)_3.9H_2O$ were dissolved in distilled water respectively. After this, on the basis of molar ratio, 10% excess citric acid was added to the aqueous solution of nitrates with stirring for 1 hour at 80°C. The solution was continuously stirred until it became gel. The obtained sample was dried at 120°C for overnight followed by calcinations at

600°C for 6 hours in stagnant air. In this way I have prepared various effective perovskite catalysts in the laboratory as steps mentioned in Figure 4.7.

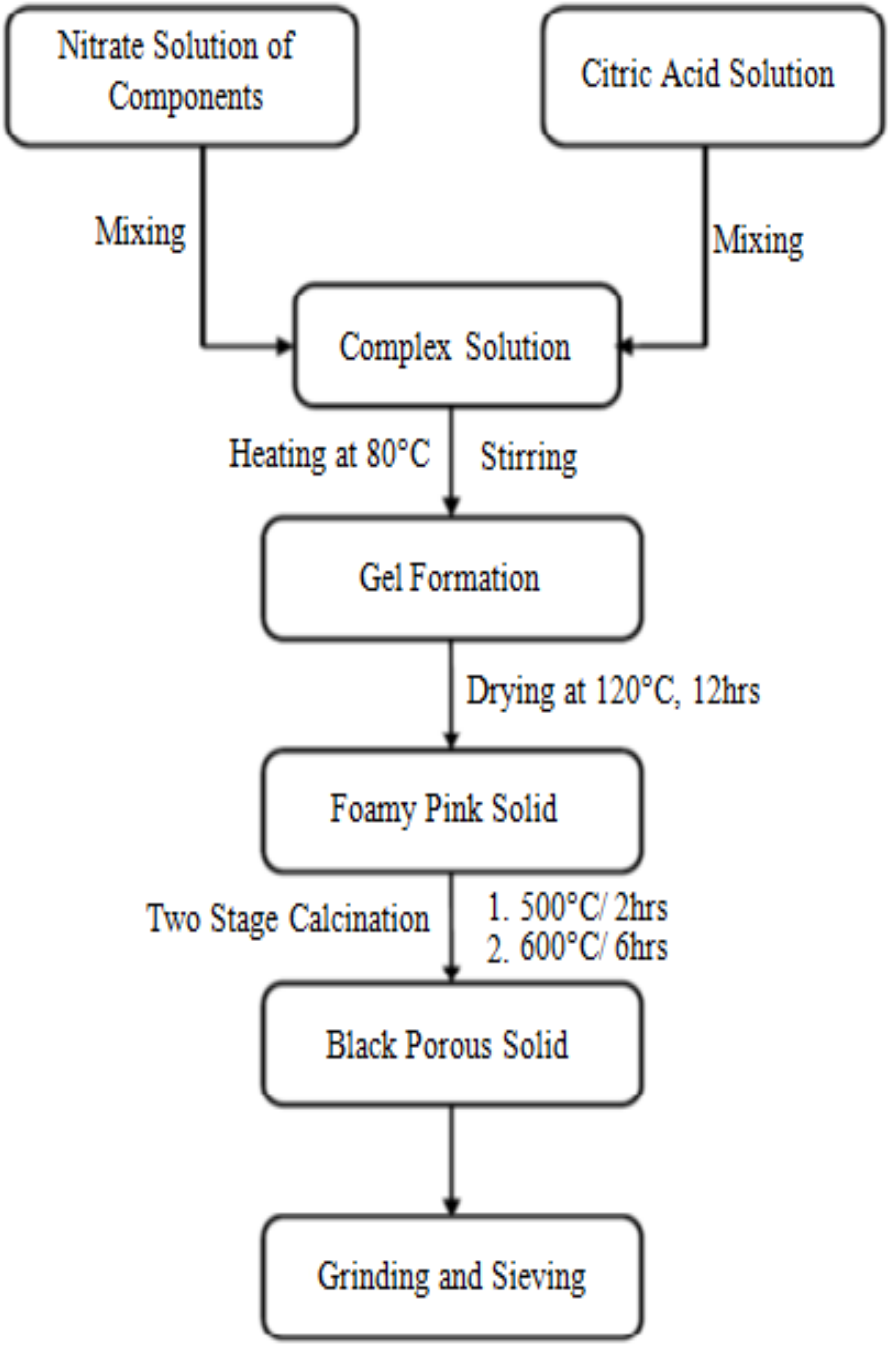

Figure 4.7 Flow diagram of Sol-gel method

Mentus *et al.*, 2007 and Wendlandt *et al.*, 2008 are studied the thermal decomposition of lanthanum nitrate and they found different pathways of decomposition

in different atmospheres. Figure 4.8 and Figure 4.9 are the TG-DTG curves of the mixed nitrates and a multi-step decomposition performance.

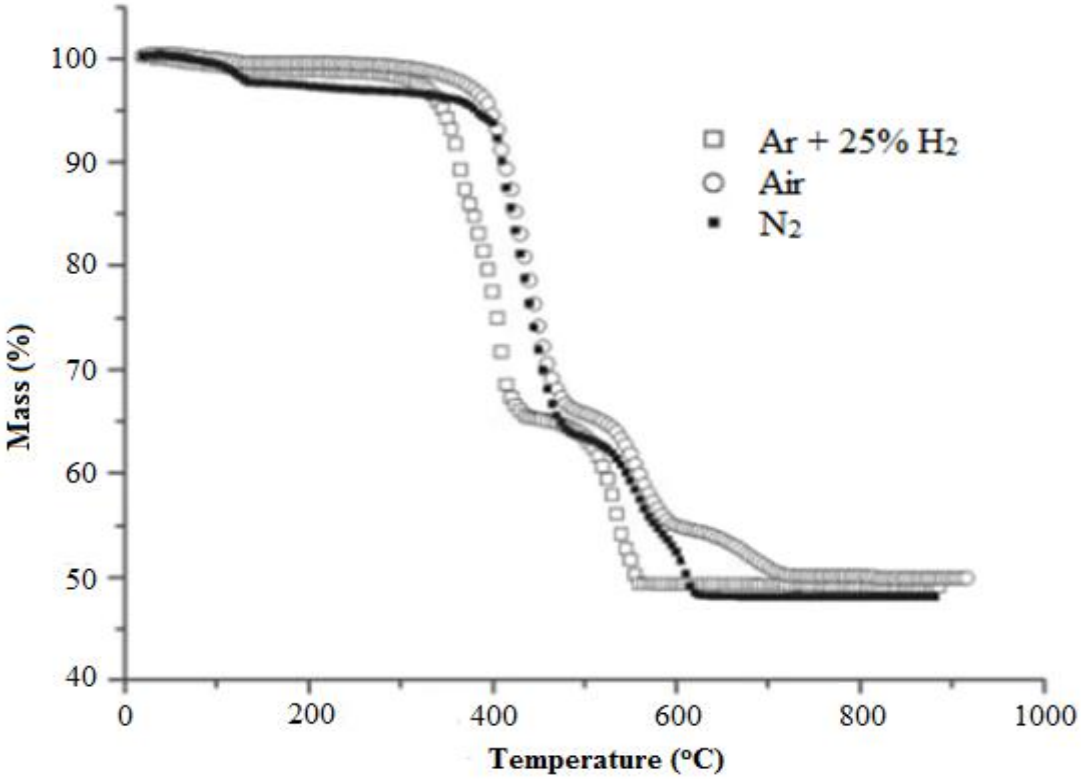

Figure 4.8 TG curves of dehydrated $La(NO_3)_3$ in different atmospheres, at heating rate 15°C min^{-1} and at gas flow rate 90 mL min^{-1}

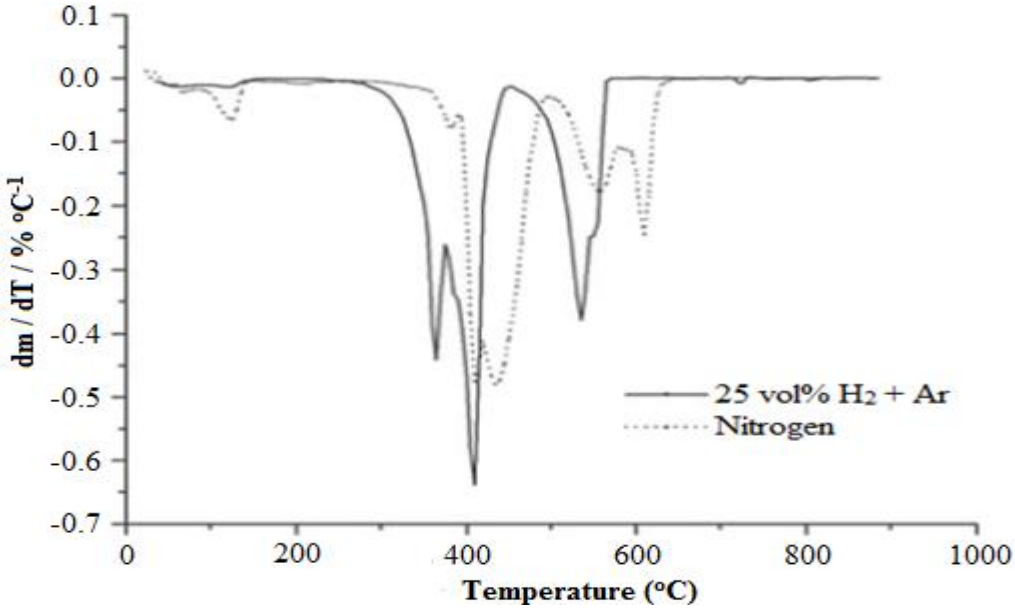

Figure 4.9 DTG curves of thermal decomposition of $La(NO_3)_3$ in nitrogen and 25% H_2 + Ar; heating rate 15°C min^{-1}, gas flow rate 90 mL min^{-1} [Mentus *et al.*, 2007]

4.2.3 Calcination Strategies of Catalysts Precursors

Calcination exposes the as prepared catalyst precursor to high temperature for the final step in the formation of finished catalysts. The primary role of calcination is to thermally decompose non-oxidic precursors, remove unwanted ligands and oxidize the support and surface species. Calcination conditions such as temperature, time and atmosphere, play dominant role in the structure and performances of the catalysts. Following calcination modes were used in the present work:

4.2.3.1 Calcination in Stagnant Air

Calcination is the conventional method of calcination done in muffle furnace in stagnant air above the decomposition temperature of constituent compounds.

4.2.3.2 Reactive Calcination

Reactive calcination of the precursor of catalysts were carried out by the introduction of low concentration of chemically reactive CO-air mixture (4.6% CO) at a total flow rate of 60 ml/min over the hot precursors. The RC was carried out in a down flow bench-scale tubular reactor having a definite amount of the precursor. The reactor was placed in a split open microprocessor temperature controlled furnace. The flow rates of CO and air were monitored using digital gas flow meters to feed the mixture (dried and CO_2 free) in required proportion to the reactor. The temperature of the precursor bed was measured with a thermocouple inserted in the thermo-well of the reactor reaching the bed. The temperature of the bed was increased at steady rate of heating at 2°C/ min from room temperature to 600°C in the flowing environment of CO-air mixture. This temperature was maintained for an hour. Then in second step of calcination temperature of the bed was increased to 750°C and maintained for another

2h under the same atmosphere followed by cooling to room temperature. The active catalyst thus obtained was stored in an air-tight bottle.

4.2.4 Nomenclature of prepared catalysts

The Nomenclature of various catalysts prepared for simultaneous catalytic removal of diesel soot & NOx emissions are given in Table 4.3.

Table 4.3 Nomenclature of prepared catalysts

Sl. No.	Catalyst Composition	Name of Catalyst	Preparation Method	Calcination Strategies
Optimization of Calcination Temp				
1.	$LaFeO_3$	LFes600	Sol-gel	600°C, 6h, Air
2.	$LaFeO_3$	LFes650	Sol-gel	650°C, 6h, Air
3.	$LaFeO_3$	LFes700	Sol-gel	700°C, 6h, Air
4.	$LaFeO_3$	LFes750	Sol-gel	750°C, 6h, Air
Optimum Calcination Temp= 700°C				
Effect of Preparation Methods				
5.	$LaFeO_3$	LFesc700	SCS	700°C, 6h, Air
6.	$LaFeO_3$	LFerg700	RG	700°C, 6h, Air
Result: Excellent Method: Sol-Gel				
7.	$LaCoO_3$	LCos700	Sol-gel	700°C, 6h, Air
8.	$LaMnO_3$	LMns700	Sol-gel	700°C, 6h, Air
Substitution With K				
9.	$La_{0.8}K_{0.2}FeO_3$	LKFes700	Sol-gel	700°C, 6h, Air
10.	$La_{0.8}K_{0.2}Fe_{0.9}Cu_{0.1}O_3$	LKFeCus700-A	Sol-gel	700°C, 6h, Air
11.	$La_{0.8}K_{0.2}Fe_{0.85}Cu_{0.15}O_3$	LKFeCus700-B	Sol-gel	700°C, 6h, Air
12.	$La_{0.8}K_{0.2}Fe_{0.8}Cu_{0.2}O_3$	LKFeCus700-C	Sol-gel	700°C, 6h, Air
13.	$La_{0.8}K_{0.2}Fe_{0.85}Co_{0.15}O_3$	LKFeCos700	Sol-gel	700°C, 6h, Air
Result- Best Composition - $La_{0.8}K_{0.2}Fe_{0.85}Cu_{0.15}O_3$				
Calcination Strategies				
11.	$La_{0.8}K_{0.2}Fe_{0.85}Cu_{0.15}O_3$	LKFeCus700-B	Sol-gel	750°C, 6h, SA

14.	$La_{0.8}K_{0.2}Fe_{0.85}Cu_{0.15}O_3$	LKFeCus700-D	Sol-gel	700°C, 6h, FA
15.	$La_{0.8}K_{0.2}Fe_{0.85}Cu_{0.15}O_3$	LKFeCus700-E	Sol-gel	700°C, 6h, RC

*SA=stagnant air, FA=flowing air, RC= Reactive calcination

4.2.5 Characterization Techniques used for Diesel Soot

The characteristics of prepared diesel soot were analyzed by proximate analysis, XRD, Particle size analysis and calorimetric analysis.

4.2.5.1 Particle size analysis

The particle size analysis of the samples were measured using the Laser diffraction (Helium-Neon Laser, 5 Milli-watt maximum output) based particle size analyzer (ANKERSMID, CIS-50, USA) relies on the fact that particles passing through a laser beam will scatter light at an angle that is directly related to their size. As particle size decreases, the observed scattering angle increases logarithmically. Scattering intensity is also dependent on particle size, diminishing with particle volume. Large particles therefore scatter light at narrow angles with high intensity whereas small particles scatter at wider angles but with low intensity.

4.2.5.2 Calorimetric Analysis

A calorimeter is an instrument used for measuring the caloric value of a fuel. A bomb calorimeter is a constant-volume reactor used to measure the heat of combustion of a solid or liquid fuel. Bomb calorimeter has to withstand the large pressure within the calorimeter as the reaction is being measured at high pressure. Electrical energy is used to ignite the fuel; as the fuel is burning, it heats up the bomb and surrounding water kept outside the calorimeter. The change in temperature of the water allows for calculating calorific value of the fuel.

The pelletized soot sample was tied with thread to a 10 cm length of fuse wire connected between the two electrodes and bomb assembly was tightened. The bomb was pressurized with pure oxygen at 25atm and it was submerged under a known volume of water (ca. 1750 ml) before the charge is electrically ignited. The switch was pushed to ignite the fuse wire and thereby thread and soot pellet. Energy is released by the combustion and heat flow crosses the stainless steel wall, thus raising the temperature of the surrounding water jacket. The temperature change in the water was then accurately measured with a temperature indicator connected to a thermo couple placed inside the calorimeter. This reading, along with a bomb factor (which is dependent on the heat capacity of the metal bomb parts), is used to calculate the energy given out by the sample burn. A small correction is made to account for the electrical energy input as the burning of fuse wire and thread. After the temperature rise has been measured, the excess pressure in the bomb is released. Schematic view of calorimeter is used in the laboratory as shown in Figure 4.10.

Figure 4.10 Schematic view of Calorimeter

Since, there is no heat exchange between the calorimeter and surroundings → Q = 0 (adiabatic); no work performed → W = 0. Thus,

The total internal energy change ΔU (total) = Q + W = 0

Also, total internal energy change ΔU (total) = ΔU (system) + ΔU (surroundings) = 0 → ΔU (system) = - ΔU (surroundings) = -Cv ΔT (constant volume → dV = 0)

Where Cv = heat capacity of the bomb

Before the bomb can be used to determine heat of combustion of any compound, it must be calibrated. The value of Cv can be estimated by

Cv (calorimeter) = m (water). Cv (water) + m (steel). Cv (steel)

m (water) and m (steel) can be measured;

Cv (water)= 1 cal/g.K

Cv (steel)= 0.1 cal/g.K

In laboratory, Cv is determined by running a compound with known heat of combustion value: Cv = Hc/ΔT, Common compounds are benzoic acid (Hc = 6318 cal/g) or p-methyl benzoic acid (Hc = 6957 cal/g).

Temperature (T) is recorded every minute and ΔT = T (final) - T (initial)

A small factor contributes to the correction of the total heat of combustion is the fuse wire. Nickel fuse wire is often used and has heat of combustion = 981.3 cal/g. In order to calibrate the bomb, a small amount (~ 1 g) of benzoic acid or p-methyl benzoic acid is weighed. A length of Nickel fuse wire (~10 cm) is weighed both before and after the combustion process.

Mass of fuse wire burned Δm = m (before) - m (after)

The combustion of sample (benzoic acid) inside the bomb, $\Delta Hc = \Delta Hc$ (benzoic acid) x m (benzoic acid) + ΔHc (Ni fuse wire) x Δm (Ni fuse wire)

$\Delta Hc = Cv. \Delta T \rightarrow Cv = \Delta Hc/\Delta T$

Once, Cv value of the bomb is determined, the bomb is ready to use to calculate heat of combustion of any compounds by $\Delta Hc = Cv. \Delta T$.

4.2.5.3 Proximate analysis

Proximate analysis of soot was done for the moisture, volatile matter (VM), ash and fixed carbon content of the soot. For moisture soot was heated for 108°C for 1h with lids of the silica crucible open. Volatile matter was determined by heating soot at 925°C for 7min in absence of air (lid close). Ash was determined by two step heating i) heating soot at 425°C for 30min in absence of air and ii) heating at 775°C in presence of air. Lastly fixed carbon was calculated by subtracting moisture, VM and ash from total weight.

4.3 Characterization Techniques used for Catalysts

The information on the structure of the catalysts provides insight into the inter-relation between the parameters of catalysts preparation and the performance of the catalyst. The catalyst characterization, i.e. the investigation of relevant aspects of the catalyst structure may also be required for quality control on the basis of previous empirical observations. The information based on characterization of the catalyst is useful for catalytic process optimization and for the manufacture of catalyst. The characterization helps to understand the inter-relationship between the activity and selectivity of a catalyst and its different physical and chemical properties. The prepared catalysts were characterized by various techniques like X-ray diffraction (XRD)

analysis, Fourier Transform Infrared Spectrum (FTIR), Scanning electron microscopy (SEM) and low temperature N_2 adsorption as given in Table 4.4.

Table 4.4 Techniques used for characterization of catalyst

Techniques Applied	Physico-Chemical Properties
Low temperature N_2 adsorption Fourier transform infrared spectroscopy (FTIR) X-ray photoelectron spectroscopy (XPS)	Textural properties: surface area, pore volume, pore size distribution, average pore diameter Infrared spectrum of absorption, emission, and Photoconductivity Elemental composition, empirical formula, chemical state
Scanning electron microscopy (SEM)	Surface structure (texture), particle size estimation
Energy-dispersive X-ray spectroscopy (EDX) X ray diffraction (XRD)	Elemental analysis Phase analysis, mean crystallite size, crystal size, crystal size distribution and lattice parameter

4.3.1 Textural Characterization by N_2-sorption

The standard method for measuring SSA is by gas adsorption and the application of the Brunauer, Emmett, and Teller (BET) equation [Brunauer *et al.*, 1938] which is described in detail in a number of reference books [Gregg and Sing, 1982, Condon 2006]. BJH analysis can also be employed to determine pore area and specific pore volume using adsorption and desorption techniques. This technique characterizes pore size distribution independent of external area due to particle size of the sample. The parameters like surface area, distribution of the sizes of pores and particles and pore shapes play a major role in governing the vital reaction parameters like catalytic activity, selectivity and stability as well as physical factors such as permeability, diffusivity, effectiveness factor and mechanical strength.

5.3.2 BET Surface Area measurements

Physisorption measurements are widely used to determine the surface area and pore size distribution of catalysts. Physisorption occurs when a gas (adsorptive) is brought in contact with an outgassed solid (adsorbent). The measurement of surface area

by nitrogen adsorption using the BET equation has been employed to characterize catalysts for many years. The theory behind the BET equation is an extension of the Langmuir model for monolayer molecular adsorption. The adsorption in the first layer is assumed to take place in an array of surface sites with uniform energy. Molecules in the first layer act as sites for multilayer adsorption, which in the simplest case approaches infinite thickness as $p \rightarrow p_0$.

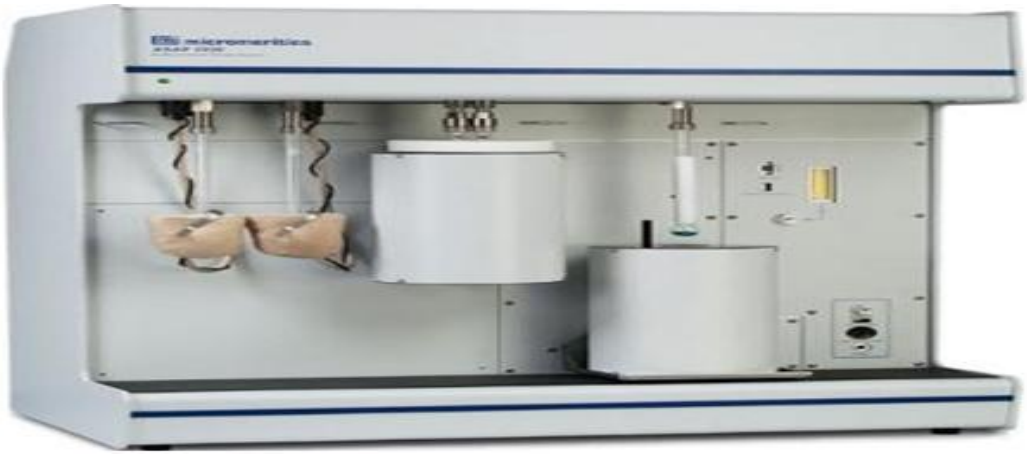

Figure 4.11 Image of BET instrument

Principle of BET analysis: The principle of BET analysis is that at low relative pressure, gas adsorbs to a solid in a monolayer (multilayers form at higher pressures) as shown Figure 4.11 by knowing the number of gas molecules in a monolayer and the dimensions of an individual molecule, the surface area covered by the monolayer can be calculated. The BET equation (Smith 1970) models a measured number of moles of adsorbate (n) adsorbed on 1 g of sample with the applied gas pressure (P) following the relationship given in Equation 4.5.

$$\frac{P}{n(P_0 - P)} = \frac{1}{n_m c} + \frac{C-1}{n_m C}\left(\frac{P}{P_o}\right) \quad BET\ equation \ldots\ldots\ldots\ldots\ldots\ldots\ldots\ldots\ldots\ldots \quad (4.5)$$

Where; n_m = calculated number of moles adsorbed as a monolayer on 1g of adsorbent (monolayer capacity),

P = Sample (gas) pressure, P_o = saturation vapor pressure of the gas,

n= amount of gas adsorbed at the relative pressure P/P_0

In Equation 4.6, C = a constant that is dependent upon the shape of the isotherm (BET constant).

$$\mathrm{C} = Exp\left(\frac{E_1 - E_2}{RT}\right) \ldots\ldots\ldots\ldots\ldots\ldots\ldots\ldots\ldots\ldots\ldots\ldots\ldots\ldots\ldots\ldots\ldots\ldots\ldots\ldots\ldots\ldots\ldots \quad (4.6)$$

E_1 is the heat of adsorption for the first layer; E_2 is that for the second and higher levels and is equal to the heat of liquefaction. n_m is obtained by plotting $P/V_a(P_o - P)$ against P/P_o, where V_a is the volume of gas adsorbed per gram of sample normalized to standard temperature and pressure (STP) (mL/g). Generally the plot is linear at low relative pressures ($P/P_o < 0.3$). The slope of the linear part of the graph has a slope (s) of c - $1/V_m c$ and an intercept (i) of $1/V_m c$, where V_m is the volume of gas required to form a monolayer on a unit gram of the sample (mL/g). Both s and i have units of cm^3/g at STP. By algebraic substitution, $V_m = (s + i)^{-1}$. Finally, the BET specific surface area (SSA) can be calculated using Equation 4.7.

$$SSA = \frac{LV_m a_m}{V_l} \ldots\ldots\ldots\ldots\ldots\ldots\ldots\ldots\ldots\ldots\ldots\ldots\ldots\ldots\ldots\ldots\ldots\ldots\ldots\ldots\ldots\ldots\ldots\ldots\ldots \quad (4.7)$$

Where; a_m = area occupied by a molecule of the N_2 adsorbate (16.2×10^{-20} m^2 for N_2),

L = Avogadro's number, and

V_l = molar volume of the analysis gas (22.4 L for N_2) at STP.

SSA= 4.35 m^2/g solid adsorbent

Brunauer-Emmett-Teller (BET) surface areas were measured at -196^{o}C using a Micromeritics ASAP 2020 Analyser in present case. Samples were degassed at 300^{o}C under vacuum prior to the measurement. The calculation of SSA was performed using

the adsorption data in the relative pressure (P/P_0) range from 0.05 to 0.35, and the total pore volume were determined from the amounts adsorbed at $P/P_0 = 0.99$. The pore size distribution curve was calculated based on the desorption curve of the isotherm using the Barrett-Joyner-Halenda (BJH) algorithm. The pore diameter was defined as the position of the maximum in the pore-size distribution.

Figure 4.12 shows an idealized form of the adsorption isotherm for phyisorption on a nonporous solid. At low pressures the surface is only partially occupied by the gas, until at higher pressures (point B on the curve) the monolyer is filled and the isotherm reaches a plateau. This part of the isotherm, from zero pressures to point B, is equivalent to the Langmuir isotherm. At higher pressures a second layer starts to form, followed by restricted multilayer formation. This is a Type II isotherm.

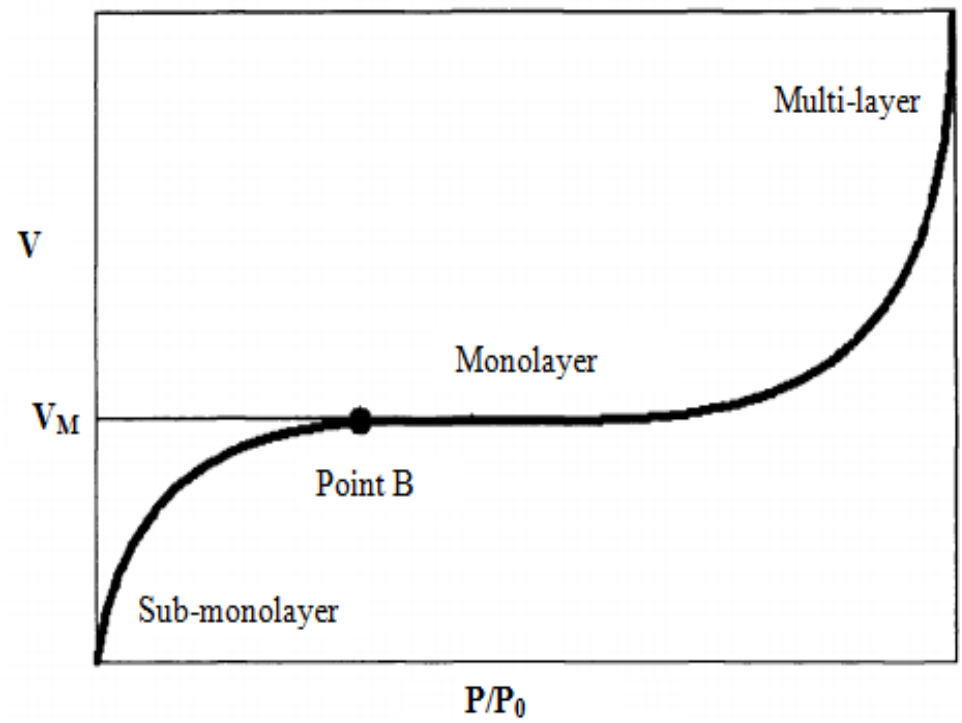

Figure 4.12 Type II isotherm

4.3.3 X-Ray Diffraction analysis

X-ray diffraction (XRD) is the most widely used and the least ambiguous method for the precise determination of the positions of atoms in all kinds of matter ranging from fluids and powders to perfect crystals. It is a non-destructive technique applied for the characterization of crystalline materials. It provides information about the structure, phases, preferred crystal orientation and other structural parameters such as lattice parameters, crystallite size, crystallite, and strain and crystal defects. The method is normally applied to data to collect in ambient conditions but in situ diffraction can be used to interpret solid state transformations under different temperatures, pressures and atmospheres. A XRD measuring instrument pictorially is presented in Figure 4.13 in center of instrumentation facility laboratory IIT (BHU) Varanasi.

Figure 4.13 XRD instrument image

Principle of X-ray Diffraction:

The technique uses a monochromatic X-ray beam incident on a finely powdered sample, comprising of an infinite amount of crystallites arranged randomly in no preferred orientation. Interaction of X-rays with the sample creates secondary diffracted beams of X-rays related to interplanar spacing's in the crystalline powder. For any set of planes the diffracted radiation forms a cone where the angle between the diffracted and

undiffracted beam is 2θ. This is defined as Bragg's Law in Equation 4.8:

$$n\lambda = 2d\sin\theta \dots\dots\dots\dots\dots\dots\dots\dots\dots\dots\dots\dots\dots\dots\dots\dots\dots\dots\dots\dots\dots(4.8)$$

Where, n is an integer, λ is the wavelength of radiation, d is the inter planar lattice spacing, θ is the Bragg angle.

X-rays are electromagnetic radiation of exactly the same nature as light but of very much shorter wavelength lying approximately in the range 0.5-2.5 Å. X-rays interact with electrons in matter. Matter absorbs X-rays in two distinct ways, by scattering and by true absorption. When a beam of X-rays impinges on the material it is scattered in various directions by the electron cloud of the atoms. If the wave length of X-rays is comparable to the separation between the atoms then interference can occur. X-ray diffraction peaks are produced by constructive interference of monochromatic light scattered by each set of lattice plans at specific angles. The peak intensities are determined by the atomic decoration in the lattice plans. For an ordered arrays of scattering centres (such as atoms or ions in a crystalline solid), this can give rise to interference maxima and minima. The analyses of the samples were carried out using a Rigaku Ultima IV X-ray diffractometer operating at 40mA and 40kV using CuKα1 radiation source (λ = 1.5405 Å). The data of 2θ from 0° to 80° were collected with a step size of 0.02. The patterns were compared with JCPDS reference data for phase identification. The Scherrer equation was used to calculate the crystallite size of the prepared samples is as follows (Equation 4.9):

$$d = \frac{0.89\lambda}{\beta cos\theta} \dots\dots\dots\dots\dots\dots\dots\dots\dots\dots\dots\dots\dots\dots\dots\dots\dots\dots(4.9)$$

Where, d, λ, θ and β are the crystallite size, X-ray wavelength (1.518 Å), Bragg diffraction angle and full width at the half maximum (FWHM) of the diffraction peak respectively.

The rays of the incident beam are always in phase and parallel up to the point at which the top beam strikes the top layer at atom B (Figure 4.14). The second beam continues to the next layer where it is scattered by atom B´. The second beam must travel the extra distance zB´ + B´z´ if the two beams are to continue travelling adjacent and parallel. This extra distance must be an integral (n) multiple of the wavelength (λ) for the phases of the two beams to be the same:

$$n\lambda = zB' + B'z'$$

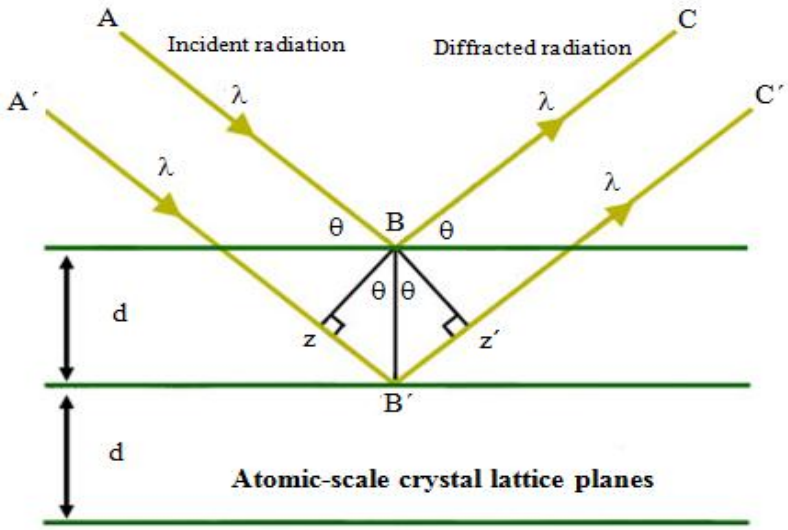

Figure 4.14 Interaction of X-ray with crystal plane for constructive interference

Recognizing d as the hypotenuse o f the right triangle BzB´, trigonometry can relate d and 0 to the distance (zB´ + B´z´). The distance zB´ is opposite θ so,

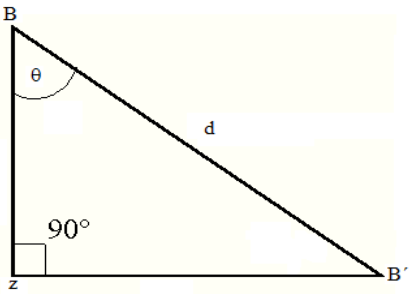

The distance zB´ is opposite θ so, zB´= d sinθ, because zB´ = B´z´, nλ=2 zB´,

Substituting, nλ = 2 d sinθ

The equation can be applied to both single crystal and crystalline powders. In the case of crystalline powders, due to the random orientation of the crystallites, the diffracted radiation forms a cone where the angle between the diffracted and undiffracted beams is 2θ.

4.3.4 Thermogravimetric Analysis – TGA

Thermogravimetric Analysis (TGA) is an analytical technique used to determine a material's thermal stability and its fraction of volatile components by monitoring the weight change as a sample is heated. Analysis relies on a high degree of precision in two measurements: weight and temperature change.

The measurement is normally carried out in air or in an inert atmosphere and the weight is recorded as a function of the increasing temperature. Changes in weight are the result of the formation of various physical and chemical bonds at elevated temperatures that lead to the evolution of volatile products or the formation of heavier reaction products.

A sample is placed into a tarred TGA sample crucible which is attached to a sensitive microbalance assembly. The sample holder portion of the TGA balance assembly is subsequently placed into a high temperature furnace. The balance assembly measures the initial sample weight at room temperature and then continuously monitors changes in sample weight (losses or gains) as heat is applied to the sample. TGA tests may be run in a heating mode at some controlled heating rate, or isothermally. Typical weight loss profiles are analyzed for the amount or percent of weight loss at any given temperature, the amount or percent of non-combusted residue at some final temperature, and the temperatures of various sample degradation processes.

4.3.5 Temperature Programmed Reduction – TPR

Temperature programmed reduction (TPR) is a technique for the determination of the reducibility of a catalyst as a function of temperature. The term TPR was first used in a paper by Robertson *et al.,* 1975 but the basic idea of characterizing catalysts by monitoring their reducibility was first suggested by Holm and Clark.

The technique involves the adaptation of the temperature programmed gas chromatograph to the purpose of measuring reduction. The catalyst can be pre-treated in different gas streams prior to the actual TPR experiment. When the sample is ready for TPR experiment the gas is switched to a gas of composition 10% H_2/balance Ar and this passes through one arm of the thermal conductivity detector then through the reactor and via a series of traps (to remove reduction products) through the other arm of the thermal conductivity detector, where the change in hydrogen concentration of the gas stream brought about by any reduction process, is monitored via the thermal conductivity change. H_2 and Ar have widely different thermal conductivities.

The gas flow is constant meaning that the change in hydrogen concentration is proportional to the rate of catalyst reduction. Distinct reducible species in the catalyst show up as peaks in the TPR spectrum.

Analysis was performed using a Thermo TPDRO 1100. The machine is designed to perform several experiments including pulse chemisorption, temperature programmed reduction, desorption and oxidation.

The sample (110 mg) was suspended in a plug of silica wool in a straight wall sample tube. The sample tube is loaded into the furnace. The sample is degassed in Ar for lh prior to analysis. The TPDRO machine is controlled by a PC, which is loaded

with reaction conditions that operate during analysis. The sample is heated from ambient temperature to 700°C at a rate of 10°C/min. The reducing gas used was a mixture of 10% H_2 in balance Ar.

4.3.6 Spectral characterization by FTIR and XPS

FTIR and XPS instruments were used for spectral characterization of the catalyst samples.

(i) FTIR spectrometer

Infrared spectroscopy has been a useful technique for materials analysis. An infrared spectrum represents a fingerprint of a sample with absorption peaks which correspond to the frequencies of vibrations between the bonds of the atoms making up the material. Because each different material is a unique combination of atoms, no two compounds produce the exact same infrared spectrum. Therefore, infrared spectroscopy can result in a positive identification (qualitative analysis) of every different kind of material. In addition, the size of the peaks in the spectrum is a direct indication of the amount of material present. With modern software algorithms, infrared is an excellent tool for quantitative analysis. It can identify unknown materials and determine the quality or consistency of a sample.

Figure 4.15 FTIR spectrometer image

Principle of FTIR: In FTIR, a single optical device called interferometer is used (Figure 4.15). Most interferometers are employing a beam splitter which takes the incoming infrared beam and divides it into two optical beams. One beam reflects off of a flat mirror which is fixed in place. The other beam reflects off of a flat mirror which is on a mechanism that allows the mirror to move a very short distance (typically a few millimetres) away from the beam splitter. The two beams reflect off of their respective mirrors and are recombined when they meet back at the beam splitter. Because the path that one beam travels is a fixed length and the other is constantly changing as its mirror moves, the signal which exits the interferometer is the result of these two beams "interfering" with each other. The resulting signal is called an interferogram which has the unique property that every data point (a function of the moving mirror position) which makes up the signal has information about every infrared frequency which comes from the source**.** Here, FTIR spectra were recorded in the range of 400-4000 cm^{-1} on Shimadzu 8400 FTIR spectrometer with KBr pellets. The infrared spectra were recorded at room temperature of the samples.

(ii) X-ray photoelectron spectroscopy (XPS)

XPS is a quantitative spectroscopic technique that measures the elemental composition of the surface, empirical formula of pure materials, chemical state and electronic state of the elements that exist within the material, elements that contaminate a surface, uniformity of elemental composition across top surface (Figure 4.16).

Figure 4.16 Image of XPS instrument

Principle of XPS: It is an electron spectroscopic method that uses X-rays to eject electrons from inner-shell orbital. The kinetic energy, E_k, of these photoelectrons is determined by the energy of X-ray radiation, h_v, and the electron binding energy, E_b, as given by Equation 4.10.

$$E_k = h\nu - E_b \quad \ldots\ldots (4.10)$$

The experimentally measured energies of the photoelectrons are given by Equation 4.11.

$$E_k = h\nu - E_b - E_w \quad \ldots\ldots (4.11)$$

Where E_w is the work function of the spectrometer.

The electron binding energies are dependent on the chemical environment of the atom, making XPS useful to identify the oxidation state and ligands of an atom. Ejected electrons can escape only from a depth of approximately 3 nm or less, making electron spectroscopy most useful to study surfaces of solid materials. In present work, XPS was

performed on an Amicus spectrometer equipped with Mg Kα X-ray radiation. For typical analysis, the source was operated at a voltage of 15 kV and current of 12 mA. Pressure in the analysis chamber was less than 10^{-5} Pa. The binding energy scale was calibrated by setting the main C 1s line of adventitious impurities at 284.7 eV, giving an uncertainty in peak positions of ±0.2 eV.

4.3.7 Morphological characterization by SEM-EDX

The scanning electron microscope (SEM) is a form of electron microscope with high magnification, large depth of focus, good resolution and ease of sample preparation. Morphological characterization was performed by using scanning electron microscopy (SEM) (Figure 4.17). SEM is used to estimate the average aggregate size, crystallinity degree of the oxides and the microstructures of the powders. SEM analysis is considered as "non-destructive"; i.e. x-rays generated by electron interactions do not lead to volume loss of the sample, so it is possible to analyze the same materials repeatedly. Topographical images in a SEM are formed from back-scattered primary or low-energy secondary electrons. The best resolution is about 2-5 nm but many routine studies are satisfied with a lower value and exploit the case of image interpretation and the extrordinary depth of field to obtain a comprehensive view of the spccimen. With non-crystalline catalysts, SEM is especially useful for examining the distribution and sizes of mesopores.

Figure 4.17 Image of SEM instrument

Principle of SEM: In basic scanning electron microscopy (SEM), a beam of highly energetic (0.1-50 keV) electrons is focused by one or two condenser lenses into a beam with a very fine focal spot (1-5nm). The beam passes through pairs of scanning coils in the objective lens, which deflect the beam horizontally and vertically so that it scans in a raster fashion over a rectangular area of the sample surface. The energy exchanges between the electron beam and the sample results in the emission of secondary electrons and electromagnetic radiation, which can be detected to produce an image. In the SEM, electrons from the electron gun are focused to a small spot, 50-100Å in diameter, on the surface of the sample. Accelerated electrons in an SEM carry significant amounts of kinetic energy, and the energy is dissipated as a variety of signals produced by electron-sample interactions when the incident electrons are decelerated in the solid sample. These signals include secondary electrons (that produce SEM images), back-scattered electrons (BSE), diffracted back-scattered electrons (EBSD that are used to determine crystal structures), photons (characteristic X-rays that are used for elemental analysis and continuum X-rays), visible light and heat. Secondary electrons

and backs-cattered electrons are commonly used for imaging samples. Secondary electrons are most valuable for showing morphology and topography on samples and back-scattered electrons are most valuable for illustrating contrasts in composition in multiphase samples (i.e. for rapid phase discrimination).

Energy-dispersive X-ray spectroscopy (EDX), sometimes called energy dispersive X-ray analysis (EDXA) or energy dispersive X-ray microanalysis (EDXMA), is an analytical technique used for the elemental analysis or chemical characterization of a sample (Figure 4.18).

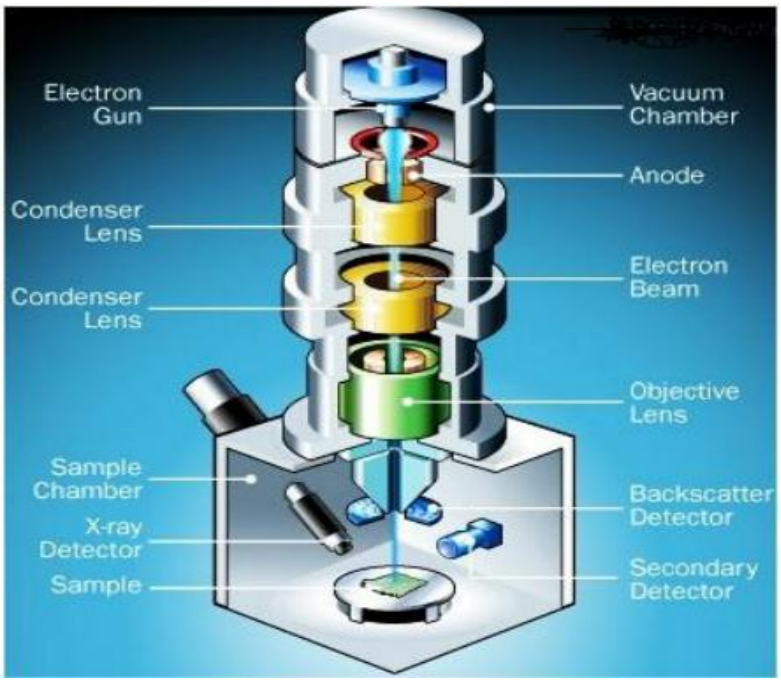

Figure 4.18 Scanning electron microscope

The electrons are detected by a type of scintillator-photomultiplier device and the resulting signal is rendered into a two-dimensional intensity distribution that can be viewed and saved as a Digital image. This process relies on a raster-scanned primary beam. The brightness of the signal depends on the number of secondary electrons reaching the detector. If the beam enters the sample perpendicular to the surface, then the activated region is uniform about the axis o f the beam and a certain number of

electrons "escape" from within the sample. As the angle of incidence increases, the "escape" distance of one side of the beam will decrease, and more secondary electrons will be emitted. Thus steep surfaces and edges tend to be brighter than flat surfaces, which results in images with a well-defined, three-dimensional appearance. The analysis was performed using a Zeiss Evo-40 Series scanning electron microscope.

Principle of EDX

It relies on an interaction of some source of X-ray excitation and a sample. Its characterization capabilities are due in large part to the fundamental principle that each element has a unique atomic structure allowing unique set of peaks on its X-ray emission spectrum [Goldstein *et al., 2003*]. To stimulate the emission of characteristic X-rays from a specimen, a high-energy beam of charged particles such as electrons or protons (see PIXE), or a beam of X-rays, is focused into the sample being studied. At rest, an atom within the sample contains ground state (or unexcited) electrons in discrete energy levels or electron shells bound to the nucleus. The incident beam may excite an electron in an inner shell, ejecting it from the shell while creating an electron hole where the electron was present. An electron from an outer, higher-energy shell then fills the hole, and the difference in energy between the higher-energy shell and the lower energy shell may be released in the form of an X-ray. The number and energy of the X-rays emitted from a specimen can be measured by an energy-dispersive spectrometer. As the energies of the X-rays are characteristic of the difference in energy between the two shells and of the atomic structure of the emitting element, EDS allows the elemental composition of the specimen to be measured [*Goldstein 2003*]. In present study, the surface morphology was determined with FEI Quanta 200 SEM instrument as well as Zeiss EVO 18 SEM-EDX instrument. An accelarating voltage of 30kV and magnification of 10000 and 20000x was applied.

Energy dispersive X-ray spectroscopy (EDX/EDS) is a chemical microanalysis technique performed in conjunction with a scanning electron microscope (SEM) as shown in Figure 4.19. An electron beam strikes the surface of a conducting sample. The energy of the beam is typically in the range 10-20keV.

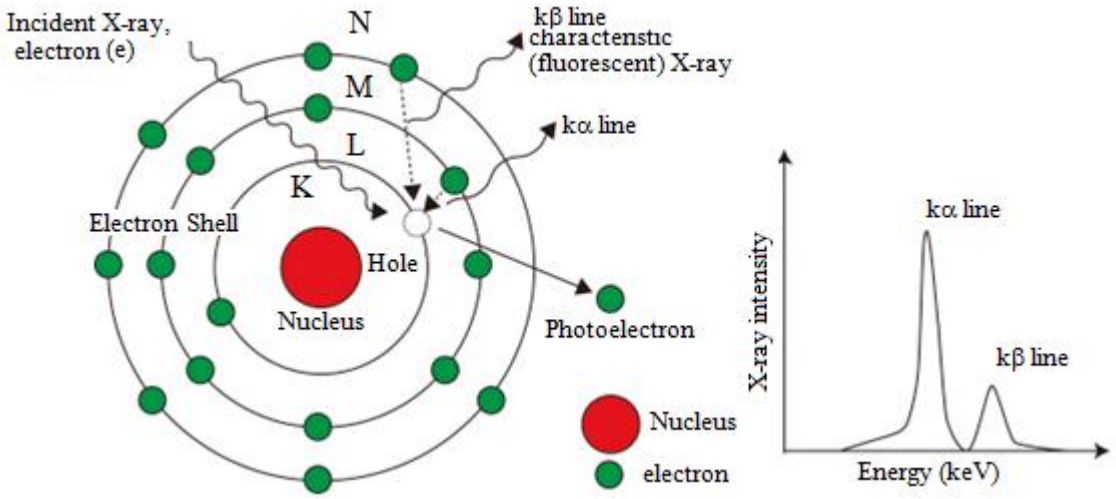

Figure 4.19 The mechanism of characteristic X-ray generation

An electron beam is aimed down into the sample to be characterised. At rest, an atom within the sample contains ground state electrons situated in concentric shells around the nucleus. The incident beam, however, excites an electron in an inner shell, prompting its ejection and resulting in the formation of an electron hole within the atom's electronic structure. An electron from an outer, higher-energy shell then fills the hole, and the excess energy of that electron is released in the form of an X-ray.

4.3.8 TEM (Transmission Electron Microscopy)

The first TEM was demonstrated by Max Knoll and Ernst Ruska in 1931, with this group developing the first TEM with resolution greater than that of light in 1933 and the first commercial TEM in 1939. Microstructures in heterogeneous catalysts are closely related to the catalytic properties. TEM and related microanalytic techniques are powerful tools in characterizing catalysts at atomic level. Application of transmission

electron microscopy (TEM) techniques on heterogeneous catalysis covers a wide range of solid catalysts, including supported metal particles, transition metal oxides, zeolites and carbon nanotubes and nanofibers etc.

TPR is a technique which can be used to determine the number of reducible species present in a material and to reveal the temperature at which reduction occurs. An important aspect of TPR analysis is that the sample need not have any special characteristics other than containing reducible metals.

The TPR analysis begins by flowing the analysis gas (typically a blend of two gases with vastly different thermal conductivities), in this case 10% H_2 in Ar, through the sample at ambient temperature to establish a base line reading. While the gas is flowing the temperature of the sample is increased linearly with time (10°C min^{-1}) and the consumption of H_2 by adsorption/reaction is monitored. Hydrogen reacts with the oxygen in the sample to form H_2O which is then trapped in the cold trap, changing the composition of the gas passing over the detector and hence its thermal conductivity. Since argon has a lower thermal conductivity than H_2, the thermal conductivity of the gas blend consequently decreases. The flowing gas removes heat from the filament more slowly, requiring less electricity to maintain a constant filament temperature. The instrument records the electrical demand as it changes. The detector signal is recorded over a range of temperatures, when these are graphed, the data forms one of move peaks.

Equipment The AutoChem 2910 Automated Catalyst Characterisation System-A catalyst was able to perform an array of high precision temperature programmed and chemisorption studies including pulse chemisorption, temperature programmed

reduction (TPR), desorption (TPD), oxidation (TPO), and reaction analyses as well as BET surface area measurements.

TPR Procedure Typically, the catalyst (110 mg) was weighed and suspended on a plug of silica wool in the U-shaped TPR sample tube. The tube was loaded in to the AutoChem 2910 analyzer and reaction parameters including sample weight, flow rates and temperature ramping rates. Typically, the catalyst was heated from ambient through to 450°C at 10°C/min while under the flow of a reducing gas mixture of 10% H_2 in argon. Changes in the reactant gas stream on reaction with the catalyst surface were detected by TCD.

4.4 Catalytic Activity Test

4.4.1 Soot-catalyst contacts

The catalytic oxidation of soot was studied under tight contact and loose contact by following mixing procedures:

(i) Tight contact

For tight contact the soot-catalyst mixture, in an appropriate ratio, was milled in an agate mortar for 15 min.

(ii) Loose contact

The soot-catalyst mixture, in an appropriate ratio, was mixed with a spatula for "loose contact". Loose contact mode represents near real contact of soot and catalyst in a DPF.

4.4.2 Experimental set-up

The experimental setup used for the catalytic activity measurement in the present study is shown in Figure 4.20. It can be divided into following three sections:

i) Air /O_2 feeding section,

ii) Reaction section, and

iii) Reactants and product analysis section.

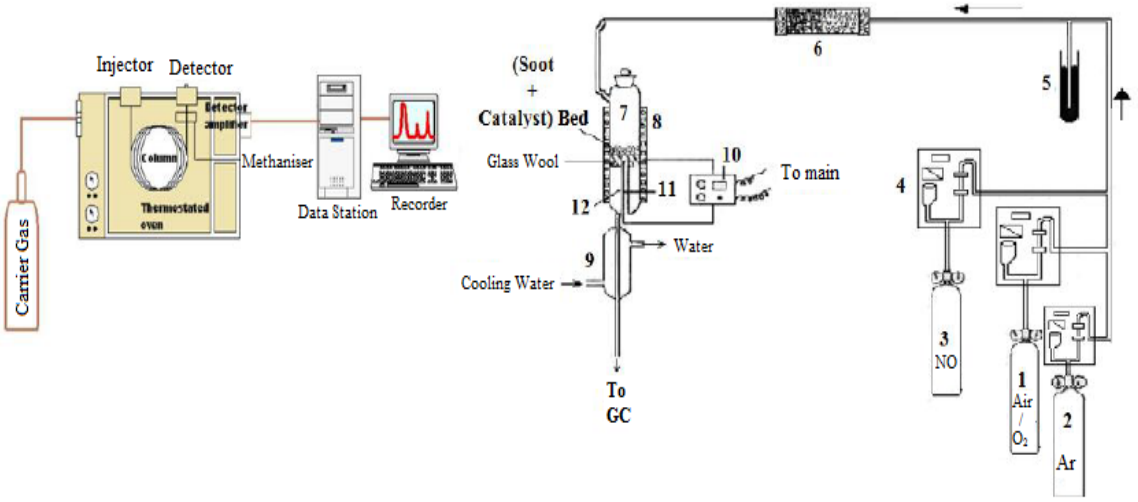

1. Air/O_2 cylinder, 2. N_2 cylinder, 3. Ar cylinder, 4. Digital gas flow meter, 5. Hg safety device, 6. Moisture and CO_2 trap, 7. Reactor, 8. Split-open furnance, 9. Condenser, 10. Temperature indicator controller, 11. Themocouple, 12. Thermocouple well.

$$C_nH_m\,(\text{Soot}) + \left(2n + \frac{m}{2}\right) NO\,(g) \longrightarrow \left(n + \frac{m}{4}\right) N_2(g) + nCO_2(g) + \left(\frac{m}{2}\right) H_2O\,(g)$$

Figure 4.20 Schematic diagram of experimental setup

(i) Air feeding section

Air from compressed cylinder was fed to the reactor, after purifying free from moisture and CO_2 by passing through a tower packed with CaO and KOH pellets. The air was monitored with the help of digital gas flow meter. A safety device in the form of mercury sealing was provided in the feeding line to check any pressure build up**.**

(ii) Reaction section

The catalytic performance of the prepared catalyst for oxidation of soot was evaluated in a compact fixed bed tubular quartz reactor. The reactor was consisting of two co-axial tubes of 20 mm and 50 mm diameter. A helical coil of quartz tube in between the co-axial tubes served as a pre-heater of the air. There is a hole in the lower part of the outer tube, to take care of breakage due to the expansion or contraction of air in between co-axial tubes as the unit is subjected to the variation of temperature from

ambient to the reaction temperature. The pre-heated air enters the catalyst bed, kept in the inner tube as shown in the Figure 4.21. The product stream from the bottom of the reactor is cooled in a condenser to the ambient temperature and then analyzed with the help of an online Gas chromatograph.

The reactor was mounted vertically in a split open furnace. The down flow stream of air was used to avoid any distortion of the bed. The soot-catalyst (catalyst bed diameter 20 mm and height 1.27 mm) was placed on a thin layer of quartz wool which is supported on perforated quartz disc inside the inner tube. A thermocouple-well made of 4mm diameter tube was inserted axially from the bottom all the way to the centre of the disc for temperature measurement and control. The catalytic activity was evaluated by placing in the reactor a mixture of 110 mg catalyst-soot (10/1 wt. ratio) under tight/loose contact and the air oxidation was carried out in the temperature range from ambient to total conversion of soot at a constant heating rate of $1^{o}C\ min^{-1}$. The inlet air free from moisture and CO_2 was fed to the reactor with a steady flow rate of 150 ml. min^{-1}. The General view of the experiment assembly is shown in Figure 4.21- 4.23.

Figure 4.21 General view of the experiment assembly

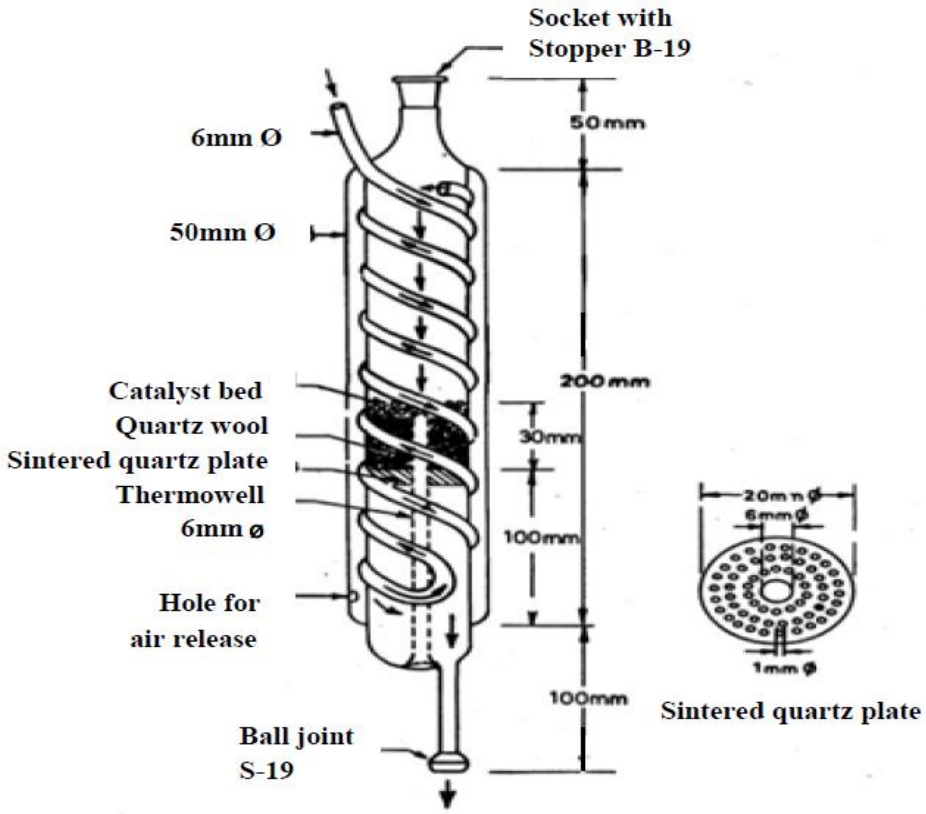

Figure 4.22 Schematic diagram of the Reactor

4.4.2.1 Reactants/ Product Analysis Section

The reactor outlet cooled gases were analyzed for CO and CO_2 by an on-line gas chromatograph equipped with methanizer using a porapak Q-column and FID detector; maintaining oven, injector and detector temperatures at 60, 80 and 80^{o}C respectively.

Figure 4.23 General view of the gas chromatograph

4.4.3 Gas Chromatograph (GC)

A gas chromatograph (GC) is an analytical instrument that measures the content of various components in a sample. The analysis performed by a gas chromatograph is called gas chromatography.

Principle of gas chromatography: The sample solution injected into the instrument enters a gas stream which transports the sample into a separation tube known as the "column." (Helium or nitrogen is used as the so-called carrier gas). The various components are separated inside the column. The detector measures the quantity of the components that exit the column. To measure a sample with an unknown concentration, a standard sample with known concentration is injected into the instrument. The standard sample peak retention time (appearance time) and area are compared to the test sample to calculate the concentration. In the present work 5765 Nucon Gas Chromatograph was used as shown in Figure 4.24. The various instrumental components used in GC are mentioned below:

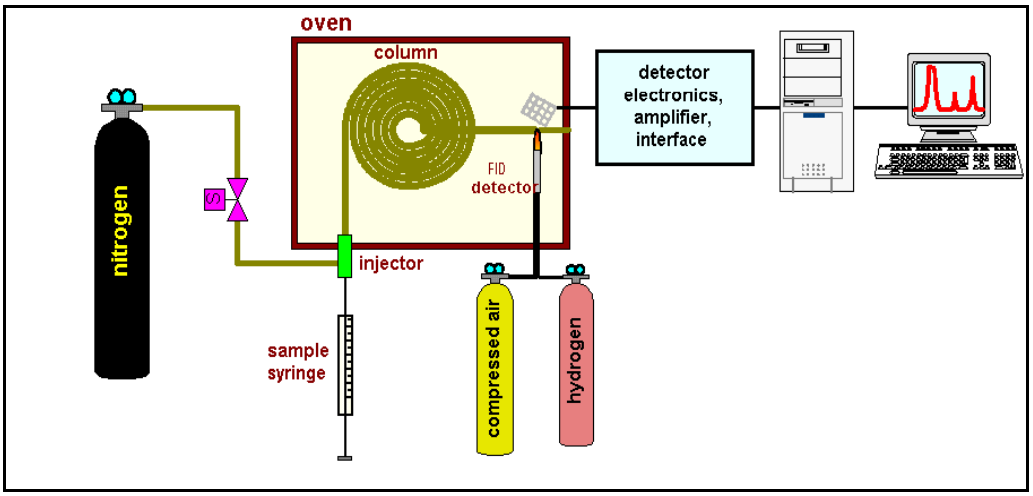

Figure 4.24 Schematic diagram of gas chromatograph

Carrier gas: The carrier gas must be chemically inert. Commonly used gases include nitrogen, helium, argon, and carbon dioxide. The choice of carrier gas is often

dependent upon the type of detector which is used. The carrier gas system also contains a molecular sieve to remove water and other impurities.

Sample injection port: For optimum column efficiency, the sample should not be too large, and should be introduced onto the column as a "plug" of vapors - slow injection of large samples causes band broadening and loss of resolution. The most common injection method is where a micro syringe is used to inject sample through a rubber septum into a flash vaporizer port at the head of the column. The temperature of the sample port is usually about 50°C higher than the boiling point of the least volatile component of the sample. For packed columns, sample size ranges from tenths of a micro liter up to 20 micro liters. Capillary columns, on the other hand, need much less sample, typically around 10^{-3} m. For capillary GC, split/split less injection is used as shown in Figure 4.25.

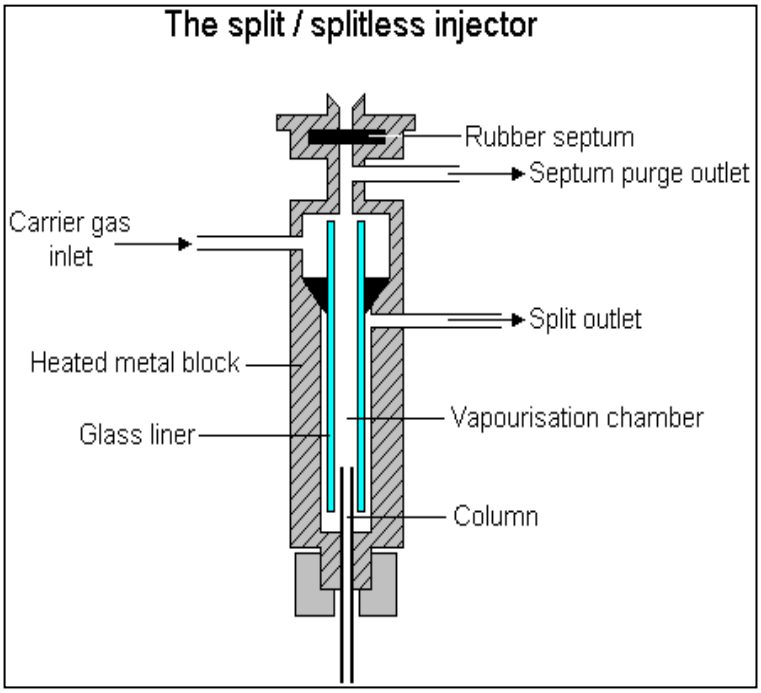

Figure 4.25 Injector diagram for gas chromatograph

The injector can be used in one of two modes; split or split less. The injector contains a heated chamber containing a glass liner into which the sample is injected through the septum. The carrier gas enters the chamber and can leave by three routes (when the injector is in split mode). The sample vaporizes to form a mixture of carrier gas, vaporized solvent and vaporized solutes. A proportion of the mixture passes onto the column, but most exits through the split outlet. The septum purge outlet prevents septum bleed components from entering the column.

Columns: For precise work, column temperature must be controlled to within tenths of a degree. The optimum column temperature is dependent upon the boiling point of the sample. As a rule of thumb, a temperature slightly above the average boiling point of the sample results in an elution time of 2-30 minutes. Minimal temperatures give good resolution, but increase elution times. If a sample has a wide boiling range, then temperature programming can be useful. The column temperature is increased (either continuously or in steps) as separation proceeds.

Detectors: The most commonly used detectors are the flame ionization detector (FID) and the thermal conductivity detector (TCD). Both are sensitive to a wide range of components, and both work over a wide range of concentrations. While TCDs are essentially universal and can be used to detect any component other than the carrier gas (as long as their thermal conductivities are different from that of the carrier gas, at detector temperature), FIDs are sensitive primarily to hydrocarbons, and are more sensitive to them than TCD. However, a FID cannot detect water. Both detectors are also quite robust. Since TCD is non-destructive, it can be operated in-series before a FID (destructive), thus providing complementary detection of the same analyzes.

Thermal Conductivity detector (TCD)

This common detector relies on the thermal conductivity of matter passing around a tungsten-rhenium filament with a current traveling through it [Harris *et al.*, 1999]. Helium or nitrogen serve as the carrier gas because of their relatively high thermal conductivity which keep the filament cool and maintain uniform resistivity and electrical efficiency of the filament. However, when analyte molecules elute from the column, mixed with carrier gas, the thermal conductivity decreases and this causes a detector response [Higson 2004]. The response is due to the decreased thermal conductivity causing an increase in filament temperature and resistivity resulting in fluctuations in voltage. Detector sensitivity is proportional to filament current while it is inversely proportional to the immediate environmental temperature of that detector as well as flow rate of the carrier gas.

Flame Ionization detector (FID)

The common detector electrodes are placed adjacent to a flame fueled by hydrogen / air near the exit of the column, and when carbon containing compounds exit the column they are pyrolyzed by the flame [Higson 2004]. This detector works only for organic / hydrocarbon containing compounds due to the ability of the carbons to form cations and electrons upon pyrolysis which generates a current between the electrodes. The increase in current is translated and appears as a peak in a chromatogram. FIDs have low detection limits (a few picograms per second) but they are unable to generate ions from carbonyl containing carbons [Harris 1999]. FID compatible carrier gasses include nitrogen, helium, and argon. Figure 4.26 shows the schematic diagram of the Flame ionization detector.

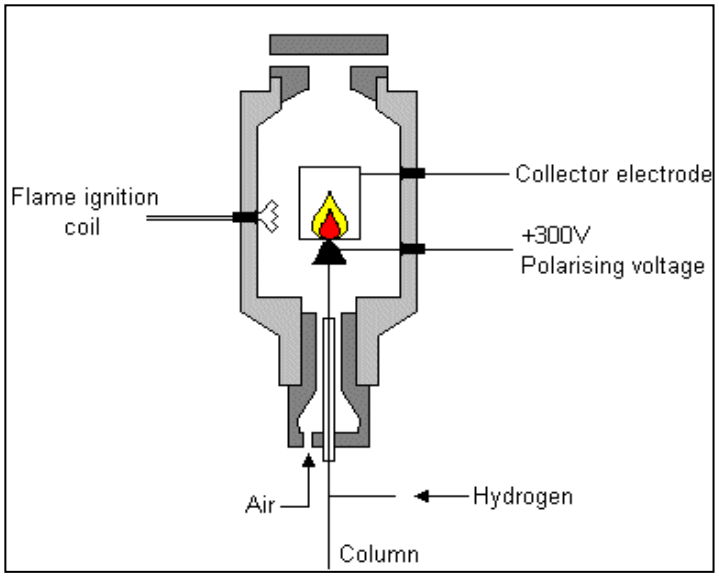

Figure 4.26 Schematic diagram of the flame ionization detector

In the GC analysis there comes a term called retention time (RT). The RT comes early (shorter) for single molecule compound, and longer for complex one. The RT is the time it takes for a compound to travel from the injection port to the detector; it is reported in minutes on our GC. Because it has to be ones adsorbed and again desorbed. There are different peaks for different compounds.

Gas Chromatography Applications

Gas chromatography is a physical separation method in where volatile mixtures are separated. It can be used in many different fields such as pharmaceuticals, cosmetics and even environmental toxins. Since the samples have to be volatile and other secretions containing large amounts of organic volatiles can be easily analyzed using GC. Knowing the amount of which compound is in a given sample gives a huge advantage in studying the effects of human health and of the environment as well. Air samples can be analyzed using GC. Most of the time, air quality control units use GC coupled with FID in order to determine the components of a given air sample. Although other detectors are useful as well, FID is the most appropriate because of its sensitivity, resolution and also because it can detect very small molecules as well. GC/MS is also

another useful method which can determine the components of a given mixture using the retention times and the abundance of the samples. This method is applied to many pharmaceutical applications such as identifying the amount of chemicals in drugs. Moreover, cosmetic manufacturers also use this method to effectively measure how much of each chemical is used for their products.

4.4.5 Reactants/products Analyzer

The reactants and the product streams to and from reactor were analyzed with the help of a NO analyzer and a gas chromatograph (GC). NO and soot conversion activities were measured by single mass flow through NO analyser GC and TPR run from 0°C to700°C at a 10°C min^{-1} rate. The catalytic activities of the all prepared catalysts were tested in a Temperature Programmed Reduction (TPR).

a. NO analyser

Technovation NO analyzer series 89 as shown in the Figure 4.27 accurately measures the concentration of gas in parts per million (ppm). These analyzers may be used as a DESK-TOP model or PANEL – MOUNTABLE. The device uses electrochemical sensors which have an enviable reputation for reliability, stability, rugged design having an electric output linearly proportional to concentration level of the gas. Ambient air monitoring can be done continuously.

Figure 4.27 General view of NO analyzer

b. Soot conversion analysis

The soot conversion activity is calculated by measuring the chromatogram areas of CO_2 peaks vs. increasing temperature. The catalytic activity was evaluated by analyzing the ignition temperature, peak temperature of soot combustion. The catalytic activity of catalyst increases as its specific SSA increases.

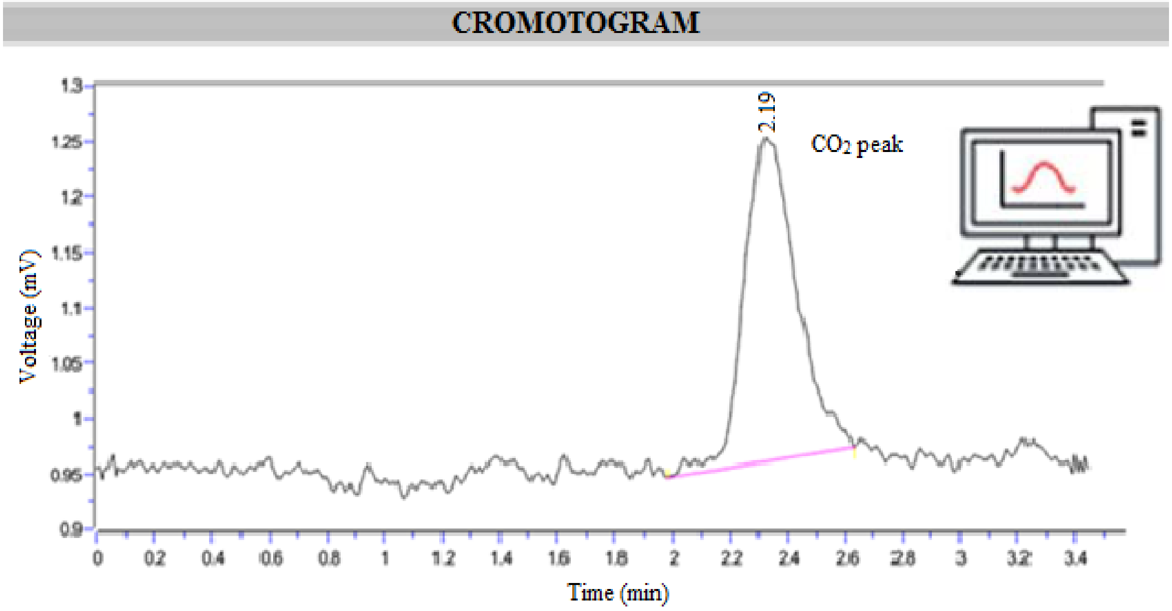

Peak No.	RT (Min)	Area (mV-Sec)	Height (mVolt)	RF	Amount (ML)	Amount%	Component Name
1	2:19	3.735	0.296	1.000	3.735	67.785	CO_2

Figure 4.28 Soot conversion to CO_2 peak in GC

4.4.4 Calculation of the soot conversion

A graph between chromatogram areas for CO_2 vs. increasing temperature for catalytic soot oxidation was plotted as shown in Figure 4.28 for a typical experimental run. The fractional conversion of soot, (α) is defined as in Equation 4.12:

$$\alpha = \frac{(M_0 - M_i)}{M_0} \ldots\ldots\ldots\ldots\ldots\ldots\ldots\ldots\ldots\ldots\ldots\ldots\ldots\ldots (4.12)$$

Where, M_o is the weight of initial soot taken and M_i is the weight of soot at temperature T_i. M_o is proportional to total area of the graph bounded between temperature of

initiation of soot oxidation (T_o) and temperature for 100% oxidation of soot (T_f), can be given as (Equation 4.13).

$$Mo \propto \sum_{T_0}^{T_f} (\Delta A_{CO_2})_i \Delta T_i \dots\dots\dots\dots\dots\dots\dots\dots\dots\dots\dots\dots (4.13)$$

M is the weight of soot at a typical temperature (T_i), higher than the temperature (T_o). The weight loss (M_o-M) at temperature T_i, which is proportional to the area bounded by the graph between T_o and T_i, can be given as (Equation 4.14)

$$(Mo - Mi) \propto \sum_{T_0}^{T_i} A_{CO_2} \Delta T \dots\dots\dots\dots\dots\dots\dots\dots\dots\dots\dots\dots (4.14)$$

Therefore, the value of X at various extent of reaction can be calculated using the following formula (Equation 4.15):

$$X_i = \sum_{T_0}^{T_i} A_{CO_2} \Delta T \Big/ \sum_{T_0}^{T_f} A_{CO_2} \Delta T \dots\dots\dots\dots\dots\dots\dots\dots\dots\dots\dots\dots (4.15)$$

Thus, the above graph (R. 3.14) can be plotted between conversions vs. temperature as shown in Figure 4.29.

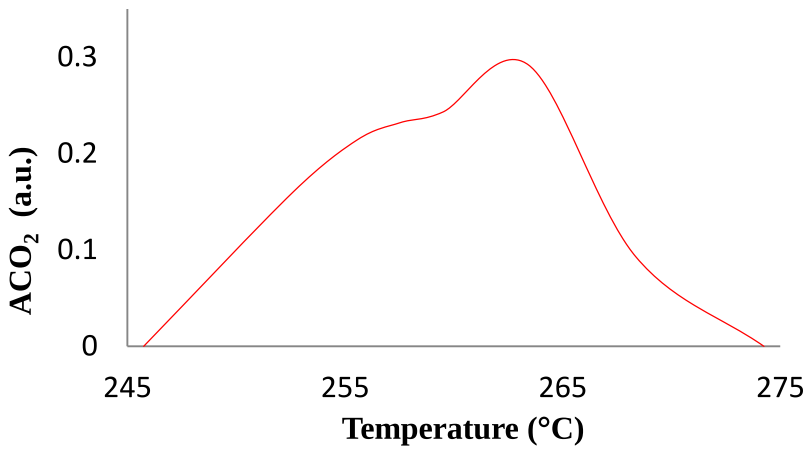

Figure 4.29 A typical plot of chromatogram area of CO_2 formed by soot oxidation vs. Temperature

4.4.5 Calculation of the NO Conversion

The conversion of NO at any instant was calculated on the basis of values of the concentration of NO in the feed, NO conversion (X_{NO}) was calculated as follows: and product stream by the following Equation 4.16:

$$X_{NO}\ (\%) = \left[1 - \frac{NO_{out}}{NO_{in}}\right] \times 100 \ldots\ldots\ldots\ldots\ldots\ldots\ldots\ldots\ldots\ldots\ldots\ldots\ldots\ldots\ldots\ldots\ldots\ldots (4.16)$$

For simultaneous removal of soot-NOx can be represented by Equation 4.17 as follows:

$$2C\ (soot) + \ 2NO + O_2 \rightarrow 2CO_2 \ldots\ldots\ldots\ldots\ldots\ldots\ldots\ldots\ldots\ldots\ldots\ldots\ldots\ldots\ldots\ldots\ldots\ldots (4.17\ )$$

From the catalytic performance measurements following parameters were derived: ignition temperature (Ti) and concentrations of CO_2, N_2 and N_2O formed. The two selectivity parameters shown below were used in order to evaluate the NOx reduction performance. The selectivity to N_2 formation (S_{N2}) corresponds to the fraction of soot used for the reduction of NO into N_2 and N_2O and that into only N_2, respectively.

Selectivity to N_2 formation can be written in terms of concentration of N_2 and other by-products (N_2 and CO_2) (Equation 4.18):

$$S_{N_2}(\%) = \left[\frac{C_{N_2}}{C_{CO_2}}\right] \times 100 \ldots\ldots\ldots\ldots\ldots\ldots\ldots\ldots\ldots\ldots\ldots\ldots\ldots\ldots\ldots\ldots\ldots\ldots\ldots\ldots\ldots\ldots (4.18)$$

Selectivity to N_2O (S_{N2O}) can be written in terms of concentration of by-products (N_2 and N_2O) to N_2O (Equation 4.19):

$$S_{N_2O}(\%) = \left[\frac{C_{N_2O}}{C_{N_2} + C_{N_2O}}\right] \times 100 \ldots\ldots\ldots\ldots\ldots\ldots\ldots\ldots\ldots\ldots\ldots\ldots\ldots\ldots\ldots\ldots\ldots\ldots\ldots\ldots\ldots\ldots (4.19)$$